Folate-targeted nanoparticle delivery of chemo- and radiotherapeutics for the treatment of ovarian cancer peritoneal metastasis

Michael E. Werner[a], **Shrirang Karve**[a], **Rohit Sukumar**[a], **Natalie D. Cummings**[a], **Jonathan A. Copp**[a], **Ronald C. Chen**[b], **Tian Zhang**[c], and **Andrew Z. Wang**[a,*]

[a]Laboratory of Nano- and Translational Medicine, Department of Radiation Oncology, Lineberger Comprehensive Cancer Center, University of North Carolina School of Medicine, Chapel Hill, NC, USA

[b]Department of Radiation Oncology, Lineberger Comprehensive Cancer Center, University of North Carolina School of Medicine, Chapel Hill, NC, USA

[c]Internal Medicine Program, Duke School of Medicine, Duke University, Durham, NC, USA

Abstract

Peritoneal metastasis is a major cause of morbidity and mortality in ovarian cancer. While intraperitoneal chemotherapy and radiotherapy have shown favorable clinical results, both are limited by their non-targeted nature. We aimed to develop a biologically targeted nanoparticle therapeutic for the treatment of ovarian cancer peritoneal metastasis. Folate-targeted nanoparticles encapsulating chemotherapy and/or radiotherapy were engineered. Paclitaxel (Ptxl) was used as the chemotherapeutic and yittrium-90 (^{90}Y) was employed as the therapeutic radioisotope. Folate was utilized as the targeting ligand as most ovarian cancers overexpress the folate receptor. Nanoparticle characterization studies showed monodispersed particles with controlled Ptxl release. Folate targeting ligand mediated the uptake of NPs into tumor cells. *In vitro* efficacy studies demonstrated folate-targeted NPs containing chemoradiotherapy was the most effective therapeutic compared to folate-targeted NPs containing a single therapeutic or any non-targeted NP therapeutics. *In vivo* efficacy studies using an ovarian peritoneal metastasis model showed that folate-targeted NP therapeutics were significantly more effective than non-targeted NP therapeutics. Among the folate-targeted therapeutics, the NP containing chemoradiotherapy appeared to be the most effective. Our results suggest that folate-targeted nanoparticles containing chemoradiotherapy have the potential as a treatment for ovarian peritoneal metastasis.

Keywords

---

*Corresponding author. NC Cancer Hospital – CB 295, 101 Manning Drive, Campus Box 7512, Chapel Hill, NC 27599, USA. Tel.: +1 919 445 5208; fax: +1 919 966 7681. andrew_wang@med.unc.edu (A.Z. Wang).

1. Introduction

Ovarian cancer is the second most common gynecologic malignancy and is the number one cause of death among women with gynecologic cancer. It is estimated that 21,880 women will be diagnosed with this disease in the United States in 2010 and approximately 13,850 patients will die from ovarian cancer [1]. In most cases, the disease has spread beyond the ovary at the time of diagnosis [2]. The most common site of ovarian cancer metastasis is the peritoneal cavity. Despite treatments, peritoneal metastases remain the main cause for morbidity and mortality in ovarian cancer [3]. Many clinical studies have evaluated intraperitoneal (IP) delivery of therapeutics for ovarian cancer. These studies have suggested that IP delivery of therapeutic agents can be effective. Intraperitoneal administration of chromic phosphate P-32 as radiotherapy has demonstrated clinical benefit after surgical debulking [4]. However, poor distribution of ^{32}P caused significant side effects including small bowel obstruction, and prevented the further use of IP radiotherapy [5]. Several randomized clinical trials have demonstrated the benefit of intraperitoneal chemotherapy [6]. Recently, a randomized phase III clinical trial showed IP cisplatin and paclitaxel (Ptxl) plus intravenous paclitaxel improves survival when compared to standard of care with intravenous cisplatin and Ptxl [7]. However, IP chemotherapy also led to significantly higher toxicities, since both tumor cells and healthy cells in the peritoneal cavity are exposed to high concentrations of chemotherapy.

One strategy to improve current IP treatment for ovarian cancer is to deliver the therapeutics in a molecularly targeted fashion. Nanoparticle drug delivery vehicles offer such unique opportunity. Advances in nanomedicine have led to the development of molecular targeted nanoparticle therapeutic carriers. These nano particle (NP) drug carriers can be targeted against cancer cells through cancer cell surface markers and deliver therapeutics to cancer cells directly [8]. Therefore, we proposed that a molecularly targeted NP that is capable of delivering therapeutics to ovarian cancer cells can potentially improve the treatment of peritoneal metastases of ovarian cancer. As a proof of principle, we engineered a nanoparticle that is capable of delivering Ptxl, a first-line chemotherapeutic agent against ovarian cancer, together with the well-established therapeutic radioisotope yttrium-90 to ovarian cancer cells [9]. Since most ovarian cancer cells overexpress the folate receptor, we utilized folate as the molecular targeting ligand against ovarian cancer cells [10]. We hypothesized that concurrent delivery of chemotherapy and radiotherapy, chemoradiation, should lead to higher therapeutic efficacy than either therapy alone.

2. Materials and methods

2.1. Materials

All chemicals were obtained from Sigma–Aldrich (St. Louis, MO) unless otherwise noted. PLGA (poly(D,L-lactide-co-glycolide)) with a 50:50 monomer ratio, ester-terminated, and viscosity of 0.72–0.92 dl/g was purchased from Durect Corporation (Pelham, AL). Soybean lecithin consisting of 90–95% phosphatidylcholine was obtained from MP Biomedicals (Solon, OH). DSPE–PEG2000–COOH (1,2-distearoyl-sn-glycero-3-phosphoethanolamine-N-carboxy(polyethylene glycol) 2000), DSPE–PEG2000–Folate (1,2-distearoyl-sn-glycero-3-phosphoethanolamine-N-carboxy(polyethylene glycol) 2000-Folate) and DMPE–

DTPA (1,2-dimyristoyl-sn-glycero-3-phosphoethanolamine-diethylene-triamine-pentaacetate) were obtained from Avanti Polar Lipids (Alabaster, AL).

2.2. Formulation and characterization of NP

PLGA–lecithin–PEG core–shell NPs (ChemoRads) were synthesized from PLGA, soybean lecithin, DMPE–DTPA and DSPE–PEG–COOH using a previously reported nanoprecipitation technique [11]. Briefly, PLGA was dissolved in acetonitrile at a concentration of 1 mg/ml. To generate folate-targeted ChemoRad NPs, (Lecithin + DMPE–DTPA)/(DSPE–PEG + DSPE-PEG-Folate) (7:3, molar ratio) with a weight ratio of 15% to the PLGA polymer was dissolved in 4% ethanol aqueous solution and heated to 65 °C. The PLGA/acetonitrile solution was then added dropwise to the heated aqueous solution under gentle stirring followed by 3 min of vortexing. The nanoparticles were allowed to self-assemble for 2 h with continuous stirring under vacuum. The NP solution was concentrated using an Amicon Ultra-4 centrifugal filter (Millipore, Billerica, MA) with a molecular weight cut-off of 20 kDa. After dialysis, PBS was added to obtain a final desired concentration. The NPs were used immediately. NP size (diameter, nm) and surface charge (ζ-potential, mV) were obtained with a ZetaPALS dynamic light scattering detector (Brookhaven Instruments Corporation, Holtsville, NY). Transmission electron microscopy (TEM) images were obtained at the Microscopy Services Laboratory Core Facility at the UNC School of Medicine.

2.3. NP Ptxl formulation, characterization and release

To prepare drug-encapsulated NPs, Ptxl at a dosage of 10% (wt/wt) of the polymer was dissolved into the PLGA/acetonitrile solution before nanoprecipitation. To measure the drug loading yield and release profile of Ptxl, 3 mL NP solutions at a concentration of 0.5 mg/mL were split equally into 30 Slide-ALyzer MINI dialysis microtubes with a molecular weight cut-off of 10 kDa (Pierce, Rockford, IL) and subject to dialysis against 4 L phosphate buffer saline (PBS) with gentle stirring at 37 °C. PBS was changed periodically during the dialysis process. At the indicated times, 0.1 mL of solution from three microtubes was removed and mixed with an equal volume of acetonitrile to dissolve the NPs. Ptxl content was subjected to quantitative analysis using an Agilent 1100 HPLC (Agilent Technologies, Santa Clara, CA) equipped with a C18 Chromolith flash column (Merck KGaA Darmstadt, Germany). Ptxl absorbance was measured by an UV–VIS detector at 204 nm and a retention time of 1.5 min in 0.25 mL/min 50:50 acetonitrile/water non-gradient mobile phase.

2.4. Radioisotope chelation

Yttrium-90 radioisotopes were purchase from Perkin Elmer (Waltham, MA). Radioisotope chelations were carried out in 1 mM ammonium citrate buffer, pH 6. Nanoparticles were incubated with yttrium and the chelation reactions were carried out in 37 °C for duration of 45 min under gentle stirring. The nanoparticles were then dialyzed in 10K MWCO cassettes (Pierce, Rockford, IL) in phosphate buffer.

2.5. Cell culture

OVCAR3 cells were acquired from the Tissue Culture Facility at the Lineberger Comprehensive Cancer Center at UNC. SW626 and SKOV-3 cells were obtained from ATCC (Manassas, VA). OVCAR-3, SW626 and SKOV-3 cells were cultured in folate-free RPMI 1640 (Gibco, Invitrogen, Carlsbad, CA) supplemented with 10% fetal bovine serum (Mediatech, Manassas, VA) and penicillin/streptomycin (Mediatech, Manassas, VA).

2.6. Fluorescence microscopy

NPs were prepared as above with the addition of 4 ug of TopFluor Cholesterol (Avanti Polar Lipids) to the PLGA/acetonitrile solution. KB cells were grown in chamber slides (LABTEK-II, Nunc/Thermo Fisher Scientific, Rochester, NY) and treated with 140 ug/ml FT-NP or NT-NP for 1 h and washed 3 times with PBS. Cells were fixed with 1.5% paraformaldahyde, permeabilized with 0.5% Triton X-100 and washed 3 times with PBS. Coverslips were mounted on the chamber slide with Prolong Gold (Molecular Probes, Invitrogen, Carlsbad, CA) for microscopy. Images were acquired with an IX 81 microscope (Olympus, Center Valley, PA) and an ORCA-R2 camera (Hamamatsu Photonics K.K., Bridgewater, NJ) at the Microscopy Services Laboratory Core Facility at the UNC School of Medicine.

2.7. Western blot

Whole cell lystaes were generated using HNTG lysis buffer. Lysates were separated on 10% poly acrylamide gels (Bio-rad) and transferred to PVDF (Millipore) for immunoblotting. Anti-α-tubulin (Sigma) and anti FRα (Genetex) were used as primary antibodies and goat anti-rabbit-HRP(Cell Signaling) was used as a secondary antibody.

2.8. Clonogenic survival assay

Cells were treated in a 10 cm dish with the targeted or non-targeted Chemorad NP formulations for 1 h and then washed 3 times with fresh media. The cells were then seeded at various densities (ranging from 750 to 10000 cells) in 25 mL flasks. After treatment, the culture flasks were incubated for 21 days in a 37 °C humidified atmosphere of 95% air and 5% CO_2. Cells were then fixed in 50% acetone/50% methanol and stained with Trypan blue. All colonies containing 50 or more cells were counted. The normalized cell surviving fraction at each dose was calculated by dividing the absolute surviving fraction or the irradiated cells by the plating efficiency, that is, the absolute surviving fraction of cells that were sham-treated with NP with no Ptxl and ^{90}Y.

2.9. Murine xenograft model of ovarian peritoneal metastasis and in vivo efficacy

Female Nu/Nu mice were injected IP with 14×10^6 SKOV-3 cells in 400 uL of 1:1 Matrigel (BD Biosciences, San Jose, CA) and RPMI (Gibco, Carlsbad CA). Tumors were grown for 3 weeks prior to treatment. Groups of 5–7 tumor bearing mice were treated IP with 500 ug folate-targeted or non-targeted NPs containing 20 ug Paclitaxel (Sigma, St Louis, MO) and/or 50 uCi of Yttirum-90 (Perkin Elmer, Shelton, CT). Animals were monitored in accordance to guidelines presented in the University of North Carolina Institutional Animal

Care and Use Committee approved protocol for this study. Animals were euthanized when tumor burden/ascites fluid reached guidelines in protocol.

2.10. Statistical analysis

The statistical analysis software SAS was utilized for survival analysis. Kaplan Meier survival analysis was performed on the *in vivo* efficacy experiment. It was also utilized to compare targeted nanoparticles vs. non-targeted nanoparticles. Kaplan Meier survival curves were generated from the analyses. We also performed log-rank tests on the treatment arms comparing them in a pair-wise fashion.

3. Results

3.1. Formulation and characterization of folate-targeted ChemoRad nanoparticle

To deliver therapeutics to ovarian intraperitoneal metastasis in a targeted fashion, we formulated a biodegradable polymer-based nanoparticle that is capable of delivering both chemotherapy and radiotherapy. This nanoparticle is based on a previously described nanoparticle platform termed ChemoRad NP [12]. In this study, the NP is comprised of a hydrophobic core of poly (lactic-co-glycolic acid) (PLGA) with a surface coated with lipids (lecithin) and an outer shell composed of lipid-polymer conjugate 1,2-distearoyl-sn-glycero-3-phosphoethanolamine-N-[(polyethylene glycol)-2000](DSPE-PEG). Paclitaxel can be loaded in the PLGA core. To incorporate therapeutic radioisotopes into the NP, a chelator bound to a lipid, DMPE–DTPA was incorporated in the lipid monolayer surface. Finally, molecular targeting was achieved through incorporation of DSPE-PEG-Folate molecules in the particle shell. Lecithin, DSPE-PEG, DSPE-PEG-Folate and DMPE–DTPA self-assemble to form the monolayer surrounding the PLGA core due to the hydrophobic–hydrophobic interactions between the PLGA polymeric core and the hydrophobic tails of the lipids (Fig. 1).

Folate-targeted ChemoRad NPs have sizes of 75 ± 10 nm and surface charges of -35 ± 5 mV. In comparison, ChemoRad NPs with no DSPE-PEG-Folate have sizes of 73 ± 6 nm and surface charges of -41 ± 6 mV. The addition of DSPE-PEG-Folate did not significantly alter the NPs' size or surface charge. The folate-targeted NPs are also monodisperse with a narrow size distribution, confirmed by dynamic light scattering (data not shown) and TEM (Fig. 2). To demonstrate that the addition of DSPE-PEG-Folate did not change the drug release profile of ChemoRad NP, Ptxl release studies were performed. Folate-targeted ChemoRad NPs indeed showed a similar controlled drug release profile as did the non-targeted ChemoRad NPs (Fig. 3).

3.2. Folate-mediated uptake of NPs by folate receptor overexpressing ovarian cancer cells

To demonstrate that folate can mediate the specific uptake of ChemRad NPs by folate receptor overexpressing ovarian cancer cells, we chose to conduct our study with ovarian carcinoma cell lines SKOV3 and SW626. SKOV3 cells overexpress the folate receptor, similar to most ovarian cancer cells, whereas SW626 cells do not overexpress the folate receptor. Expression levels of folate receptor α (FRα) were determined by western blot. We confirmed the folate receptor expression levels with SKOV3 expressing a moderate level and

SW626 expressing a very low level of FRα (Fig. 4A). To demonstrate folate-mediated specific uptake of NPs by SKOV3, fluorescently labeled non-targeted NPs (NT-NP) or folate-targeted NPs (FT-NPs) were incubated with the SKOV3 and SW626 cells. SKOV3 cells demonstrated greater uptake of FT-NP than the NT-NP control, as demonstrated by greater fluorescence (Fig. 4B). There was minimal uptake of FT-NP and NT-NPs in the SW626 cell line. This result validates that folate-targeted NPs can be preferentially taken up by folate receptor overexpressing ovarian cancer cells and enables molecularly targeted therapeutic delivery to these cancer cells.

3.3. Evaluation of folate-targeted NPs (FT-NP) containing chemo-and/or radiotherapeutics in vitro

To assess the *in vitro* efficacy of folate-targeted nanoparticles containing chemo- and/or radiotherapeutics, we utilized a clonogenic survival assay as it reflects both the effects of chemotherapy and radiotherapy. We evaluated the NPs in SKOV-3, SW626 and OVCAR-3 cells, which were treated with FT-NP containing Ptxl and/ or ^{90}Y. We utilized SW626 as a control cell line since it does not overexpress the folate receptor, whereas SKOV-3 and OVCAR-3 endogenously express FRα (Fig. 4A). Also as a control, we incubated the cells with non-targeted NPs (NT-NP) containing Ptxl and/ or ^{90}Y. As seen in Fig. 5A, the most effective therapeutic agent against SKOV-3 is the FT-NP Ptxl ^{90}Y, the targeted NP containing both chemotherapy and radiotherapy. Comparing to NT-NPs carrying the same therapeutics, FT-NPs are more effective and the results are statistically significant. Similar results are seen in OVCAR3 cells (Fig. 5B). In contrast, while FT-NPs appear to be more effective than NT-NPs, the results are not statistically significant in SW626 cells.

3.4. Evaluation of folate-targeted NPs (FT-NP) containing chemo-and/or radiotherapeutics in vivo

To demonstrate the *in vivo* efficacy of FT-NPs for the treatment of ovarian cancer peritoneal metastases, we developed a murine model of ovarian cancer peritoneal metastasis. We injected the SKOV-3 cells into the peritoneum of immune compromised female Nu/Nu mice. The SKOV-3 cells were able to grow intraperitoneally and led to diffuse peritoneal metastases, as seen in Fig. 6A (yellow arrows). Most of the mice eventually developed ascites from peritoneal metastases, similar to human ovarian cancer (Fig. 6A).

To determine FT-NP Ptxl ^{90}Y efficacy *in vivo*, mice were given a single dose of 500 ug of NP therapeutic via intraperitoneal (IP) injection. The treatment groups were: folate-targeted NPs containing Ptxl and ^{90}Y (FT-NP Ptxl ^{90}Y), folate-targeted NPs containing Ptxl only (FT-NP Ptxl), folate-targeted NPs containing ^{90}Y only (FT-NP ^{90}Y), non-targeted NPs containing Ptxl and ^{90}Y (NT-NP Ptxl ^{90}Y), non-targeted NPs containing Ptxl only (NT-NP Ptxl), and non-targeted NPs containing ^{90}Y only (NT-NP ^{90}Y). One group of mice received NPs containing no therapeutics (NT-NP) and was the negative control. Mice were kept until they developed symptoms that met euthanasia criteria or until their spontaneous death. Mice that are alive at 90 days post treatment were euthanized according to protocol. The median time to death for the control group was 56 days. No mice died immediately or soon after the administration of therapeutics. At the end of the experiment, a total of 6 animals were alive. Two were in the FT-NP Ptxl ^{90}Y group, two in the FT-NP ^{90}Y group, one in NT-NP Ptxl and

one in NT-NP ^{90}Y. These mice were also dissected to identify any residual tumors. Both of the mice in the FT-NP Ptxl ^{90}Y group and one mouse in the FT-NP ^{90}Y had no residual tumors while the other mice all had small tumors.

Kaplan Meier survival analysis was conducted on the survival results and Kaplan Meier survival curves were generated. As seen in Fig. 6, the Kaplan Meier plot showed that mice given FT-NP Ptxl ^{90}Y appear to have the best outcome. However, the differences between the groups did not reach statistical significance using Kaplan Meier analysis. Using log-rank test to compare the treatment arms in a pair-wise fashion, we are able to demonstrate FT-NP Ptxl ^{90}Y is significantly more effective than its non-targeted counterpart, with a p value of 0.01. Both the FT-NP ^{90}Y and NT-NP ^{90}Y pair and the FT-NP Ptxl and NT-NP Ptxl pair were not statistically significant, but demonstrated a trend that folate targeting increased favorable outcome. We also grouped the mice receiving folate-targeted nanoparticle therapeutics and compared them to the mice receiving non-targeted nanoparticle therapeutics. As shown in Fig. 6C, mice receiving folate-targeted nanoparticles had significantly longer survival than mice that received non-targeted nanoparticles.

4. Discussion

The aim of our study was to develop and evaluate folate-targeted nanoparticle therapeutics for the treatment of ovarian cancer intraperitoneal metastasis. We chose to deliver Ptxl as it is a first-line chemotherapeutic for the treatment of ovarian cancer. In addition to Ptxl, we also wanted to evaluate the efficacy of combined chemotherapy and radiotherapy (chemoradiotherapy) in ovarian cancer. As mentioned in the introduction, both IP chemotherapy and IP radiotherapy have both been explored clinically and lead to improved efficacy but are limited by their toxicity. Chemoradiotherapy is a new paradigm in cancer treatment and it is the standard of care for many cancers, including head and neck, esophageal, gastric, pancreatic, rectal and lung cancers [13]. Therefore, we aimed to deliver a therapeutic radioisotope, yttrium-90, in conjunction with Ptxl. We hypothesized that the co-delivery through nanoparticles can further improve efficacy.

In order to deliver both chemotherapy and radiotherapy using the same nanoparticle, we utilized the ChemoRad nanoparticles which was first described by our group [12]. We validated that the incorporation of folate targeting ligands did not change the size, charge and drug release profiles of the ChemoRad NP. We also demonstrated that the folate targeting ligand can mediate the preferential and specific uptake of NPs by folate receptor over-expressing ovarian cancer cells. It is important to note that even cells that do not overexpress the folate receptor, such as SW626, can still take up folate-targeted nanoparticles through their baseline expression of folate receptors, as evidenced by the low level fluorescence in the SW626 cells.

The *in vitro* efficacy studies confirmed our hypothesis that folate-targeted nanoparticle therapeutics are more effective than non-targeted nanoparticles. Furthermore, nanoparticles containing chemoradiotherapy are more effective than nanoparticles containing a single therapeutic, consistent with the chemoradiotherapy paradigm. The efficacy data in SW626 cells showed a similar trend to that of OVCAR3 and SKOV3 cells. This is likely due to low

level uptake of nanoparticles by SW626 cells. Despite the similar trend, the data is not statistically significant.

To demonstrate *in vivo* efficacy of folate-targeted NP therapeutics, we developed a murine ovarian cancer peritoneal metastasis model to mimic the human condition. We chose to use SKOV3 cells as they overexpress the folate receptor but somewhat less than that of OVCAR-3, therefore making our result less biased toward the folate-targeted NP therapeutics. After IP injection of SKOV3 cells, the majority of the mice developed diffuse peritoneal disease and ascites with only a small number of them developed dominant tumors. This data is consistent with our expectation and is similar to human peritoneal metastasis of ovarian cancers. The *in vivo* efficacy data demonstrated that folate-targeted nanoparticles are more effective than their non-targeted counterparts in this murine model. However, we were unable to achieve statistical significance when comparing NPs containing both chemotherapy and radiotherapy to either therapeutic alone. To achieve statistical significance, we would need much larger sample sizes. There is certainly a trend toward improved survival when treating with folate-targeted NP that encapsulate chemoradiotherapy.

5. Conclusions

We have engineered a folate-targeted nanoparticle platform that is capable of delivering chemotherapeutics and radiotherapeutics to ovarian cancer cells in a molecularly targeted fashion. We demonstrated that folate-targeted NPs are more effective than non-targeted NPs in folate receptor overexpressing ovarian cancer cells. We were also able to demonstrate the NPs' efficacy in a murine model of ovarian cancer peritoneal metastasis. We believe our results suggest that molecularly targeted nanoparticle therapeutics should be explored as a potential treatment for ovarian cancer peritoneal metastasis.

Acknowledgments

References

1. Jemal A, Siegel R, Xu J, Ward E. Cancer statistics, 2010. CA Cancer J Clin. 2010; 60:277–300. [PubMed: 20610543]

2. Cannistra SA. Cancer of the ovary. N Engl J Med. 1993; 329:1550–9. [PubMed: 8155119]

3. Lu Z, Wang J, Wientjes MG, Au JL. Intraperitoneal therapy for peritoneal cancer. Future Oncol. 2010; 6:1625–41. [PubMed: 21062160]

4. Soper JT, Wilkinson RH Jr, Bandy LC, Clarke-Pearson DL, Creasman WT. Intraperitoneal chromic phosphate P 32 as salvage therapy for persistent carcinoma of the ovary after surgical restaging. Am J Obstet Gynecol. 1987; 156:1153–8. [PubMed: 3578429]

5. Goodman A, Bornstein L, Ball H, Smith DM, Bankoff M. Chromic phosphate therapy in carcinoma of the ovary. J Am Coll Surg. 1994; 179:401–6. [PubMed: 7921388]

6. Jelovac D, Armstrong DK. Recent progress in the diagnosis and treatment of ovarian cancer. CA Cancer J Clin. 2011; 61(3):183–203. [PubMed: 21521830]

7. Armstrong DK, Bundy B, Wenzel L, Huang HQ, Baergen R, Lele S, et al. Intraperitoneal cisplatin and paclitaxel in ovarian cancer. N Engl J Med. 2006; 354:34–43. [PubMed: 16394300]

8. Wang AZ, Gu F, Zhang L, Chan JM, Radovic-Moreno A, Shaikh MR, et al. Biofunctionalized targeted nanoparticles for therapeutic applications. Expert Opin Biol Ther. 2008; 8:1063–70. [PubMed: 18613759]

9. Gisselbrecht C, Vose J, Nademanee A, Gianni AM, Nagler A. Radioimmunotherapy for stem cell transplantation in non-Hodgkin's lymphoma: in pursuit of a complete response. Oncologist. 2009; 14(2):41–51. [PubMed: 19819923]

10. Yap TA, Carden CP, Kaye SB. Beyond chemotherapy: targeted therapies in ovarian cancer. Nat Rev Cancer. 2009; 9:167–81. [PubMed: 19238149]

11. Zhang L, Chan JM, Gu FX, Rhee JW, Wang AZ, Radovic-Moreno AF, et al. Self-assembled lipid–polymer hybrid nanoparticles: a robust drug delivery platform. ACS Nano. 2008; 2:1696–702. [PubMed: 19206374]

12. Wang AZ, Yuet K, Zhang L, Gu FX, Huynh-Le M, Radovic-Moreno AF, et al. ChemoRad nanoparticles: a novel multifunctional nanoparticle platform for targeted delivery of concurrent chemoradiation. Nanomedicine (Lond). 2010; 5(3):361–8. [PubMed: 20394530]

13. Seiwert TY, Salama JK, Vokes EE. The concurrent chemoradiation paradigm–general principles. Nat Clin Pract Oncol. 2007; 4:86–100. [PubMed: 17259930]
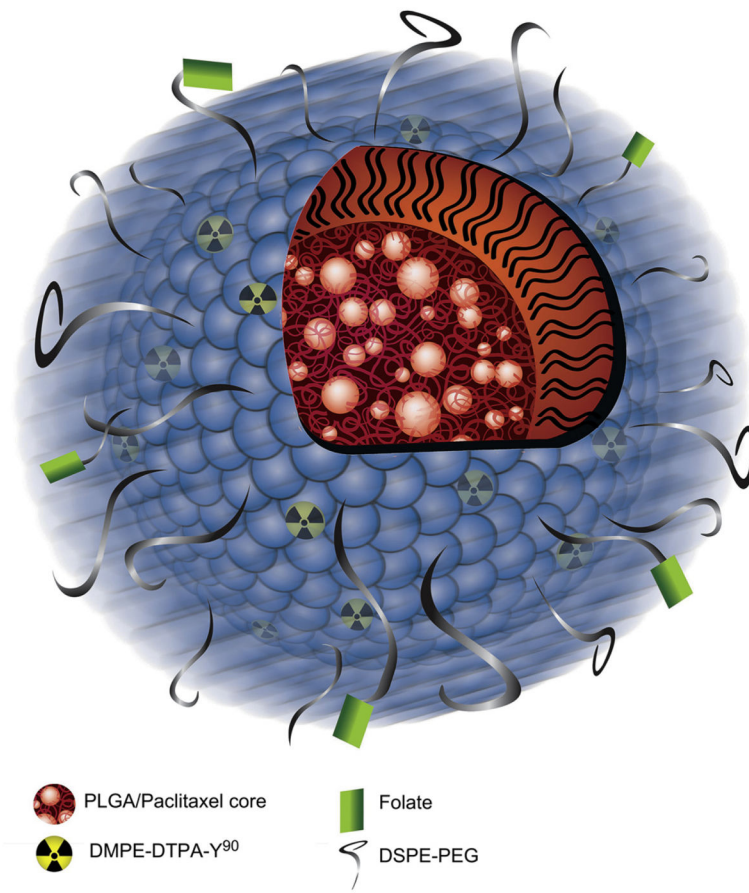
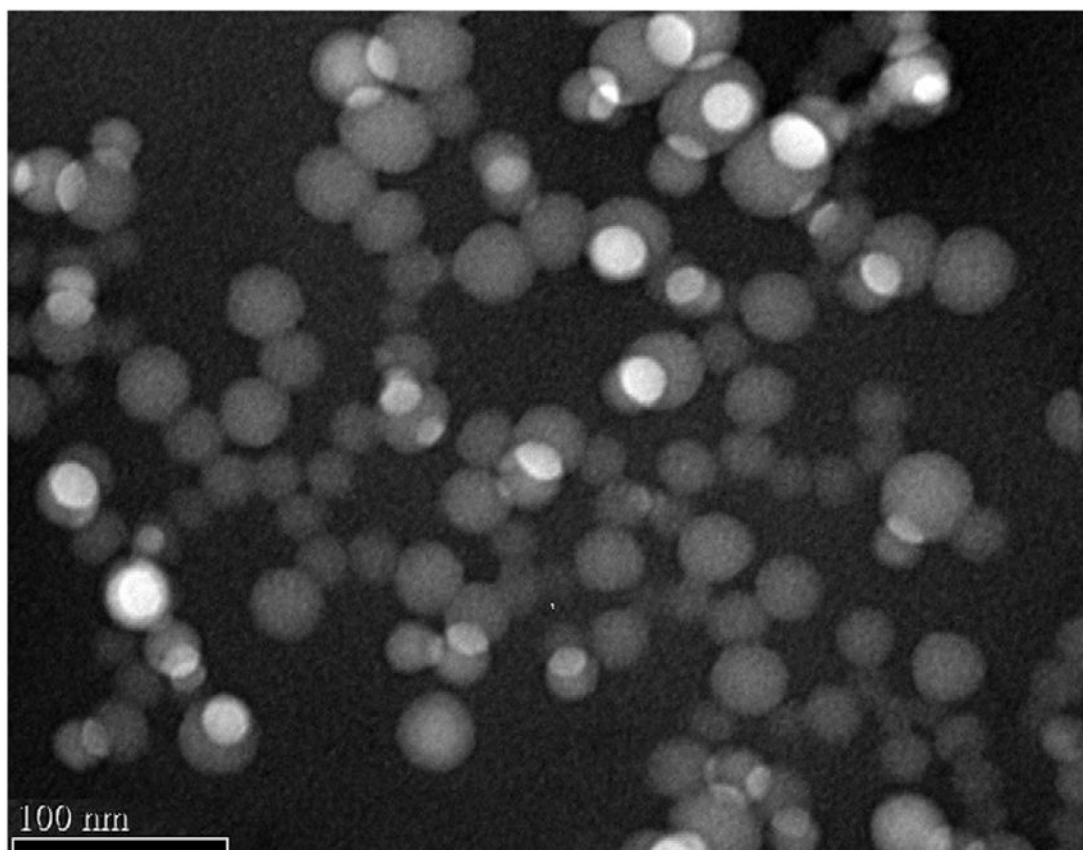**Fig. 1.**
Depiction of the folate-targeted ChemoRad NP.

Fig. 2.
TEM of the folate-targeted ChemoRad NP. Transmission Electron Micrograph of folate-targeted ChemoRad NPs showing monodisperse particles.
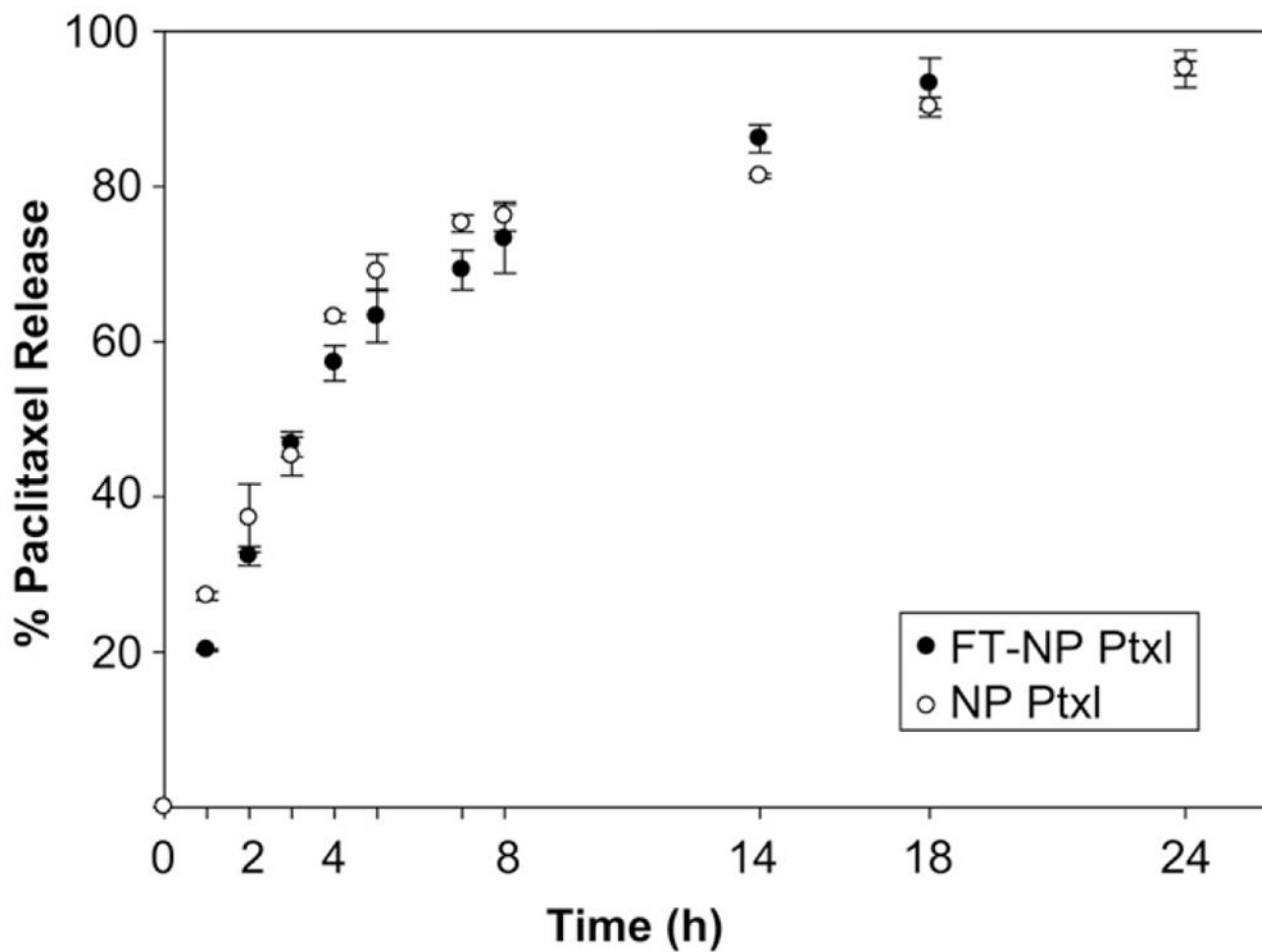
Author Manuscript

Author Manuscript

Fig. 3.
Ptxl release profiles of NPs in phosphate buffer at 37 °C. There is no significant difference in drug release between folate-targeted and non-targeted NPs. Error bars correspond to standard deviations of repeated measurements (two NP preparations, three samples per time point).
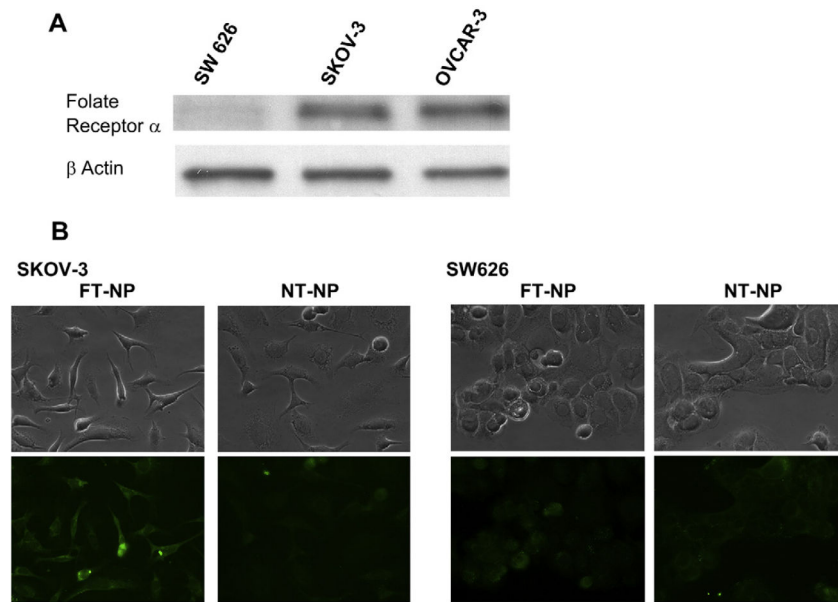
Author Manuscript

Author Manuscript

Fig. 4.
Folate-mediated intracellular uptake of NPs. A) Folate Receptor α expression levels of SW626, SKOV-3 and OVCAR-3 ovarian carcinoma cell lines were characterized by western blot. B) Representative immunofluorescent images of SKOV-3 and SW626 cells treated with NPs containing fluorescent cholesterol demonstrate greater uptake of FT-NPs (left) compared to an equal amount of NT-NP on the right.
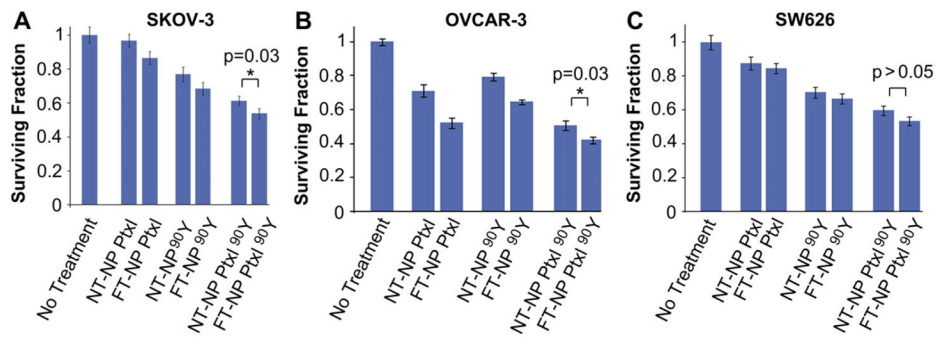
Fig. 5.

In vitro efficacy of ChemoRad NPs. Clonogenic assay results of SKOV-3 (A), OVCAR-3 (B) and SW626 (C) cells treated with various NP therapeutics. Cells treated for 1 h with 50 ug/mL of NPs containing either 20 ug of Ptxl and/or 50 uCi of Yttrium-90. *p = 0.03 using Student's *T* test.
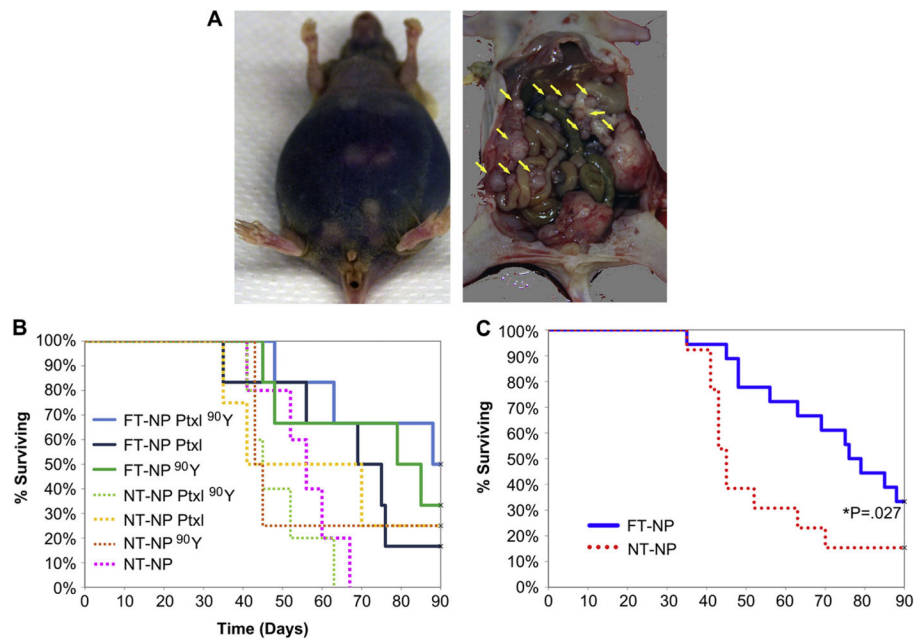
Fig. 6.

In vivo efficacy of Chemorad NPs. A) Example of murine ovarian intraperitoneal metastasis model. The mouse shown in the figure has ascites and diffuse peritoneal metastasis. B) SKOV-3 cells implanted IP in Nu/Nu female mice, 3 wk incubation prior to treatment with NPs. FT-NP Ptxl ^{90}Y appears to be the most effective treatment though statistically non-significant. C) Survival analysis comparing folate targeted NP (FT-NP) treatment arms to combined NT-NP arms (*P* = 0.027).